Buckling of Open Cylindrical Shells with Torsionally Stiff Rectangular Edge Stiffeners

G. KRISHNAMOORTHY*
San Diego State University, San Diego, Calif.

The bifurcation strength of open cylindrical shells with torsionally very stiff edge stiffeners of rectangular cross section subject to uniform axial load is determined analytically using Donnell's simplified equations. A deflection function with arbitrary undetermined coefficients satisfying the end conditions is assumed. The stress resultants are derived in terms of these coefficients. These stress resultants and the deflections of the shell are made to satisfy the assumed boundary conditions along the longitudinal edges. The resulting determinant of the equations is set equal to zero in order to obtain the critical buckling stress. The limited results obtained in this paper indicates an interesting phenomena that the critical buckling stress of a shell with a shallow edge stiffener is well above the critical buckling stress of a shell with free edges, whereas the buckling of a shell with moderate depth edge stiffeners in a narrow region is only slightly above the critical buckling stress of a shell with free edges.

Nomenclature

A_1–A_4, a_1–a_8 = arbitrary constants
A_B = area of cross section of the edge stiffener
B = half-width of the shell
b, d = width and depth of edge stiffener, see Fig. 3
$C_{i,j}$ = i, j = 1 to 4 matrix and determinant elements, see Eq. (24)
D = see Eq. (2)
E = modulus of elasticity
F_B = axial force of the edge stiffener
I_B = moment of inertia of the edge stiffener
K_x = see Eq. (2)
L = length of the shell
M_B = bending moment of the edge stiffener
M_x, M_y = bending moment per unit width of a strip in the x and y directions, respectively
m = mode number = 1, 2, 3, ...
N_x, N_y = normal forces per unit width of a strip in the x and y directions, respectively
N_{xy}, N_{yx} = shear force per unit length x and y directions, respectively
p = see Eq. (10)
R = radius to the middle surface of the cylindrical shell
R_H = horizontal reaction of the shell
r = see Eq. (11)
u, v, w = displacement in the x, y, z direction respectively
$\bar{u}, \bar{v}, \bar{w}$ = displacement in the $\bar{x}$, $\bar{y}$, $\bar{z}$ direction respectively
u_B = longitudinal displacement at the upper face of the edge stiffener, see Eq. (20)
V_B = shearing force of the edge stiffener
V_x, V_y = transverse reactions per unit width of a strip in the x and y directions, respectively
V_y' = see Eq. (17)
x, y, z = coordinate axes defined in Fig. 1
$\bar{x}, \bar{y}, \bar{z}$ = coordinate axes defined in Fig. 5
Z = see Eq. (2)
α = $m\pi/L$, see Eq. (5)
δ_v = vertical displacement at the edge of the shell and the edge stiffener, see Eq. (16)
μ = Poisson's ratio
σ_{cl} = buckling strength of a moderate length of cylindrical tube
σ_x = normal stress in the axial x direction
ϕ = see Eq. (7)
ϕ_1–ϕ_4 = indicial roots, see Eqs. (9) and (10)
ψ_0 = half subtended angle at the center of the arc of the shell, see Fig. 1

Received November 19, 1973; revision received May 31, 1974.
Index category: Structural Stability Analysis.
* Professor, Department of Civil Engineering.

Introduction

THERE is a vast amount of literature on the buckling of thin shells. A review of literature up to 1958 can be found in an article by Fung and Sechler.[1] A summary of the available solutions can be found in the *Handbook of Engineering Mechanics*[2] and the *Handbook of Structural Stability*.[3,4] Most of the literature is concerned with the buckling of a cylindrical tube.

For open cylindrical shells with edge stiffeners acting like edge beams, neither theoretical solutions nor experimental results are available. So far classical solutions based on the small deflection theory have been obtained only for curved panels with simply supported or clamped longitudinal edges subjected to shear and/or uniform axial compression.[5,6] These solutions cannot be directly applied to the structures described, since the edge conditions satisfied by these solutions are unrealistic. An exact solution of the buckling stress of cylindrical shells with free longitudinal edges subjected to uniform axial compression can be found in a paper by Chu and Krishnamoorthy.[7]

The buckling stress of an open cylindrical shell simply supported along ends with torsionally stiff edge stiffeners subject to uniform axial load is determined based on Donnell's equations.[8] A general type of deflection function with undetermined coefficients will be assumed similar to that used for investigating the buckling of cylindrical shells with free edges.[7] This type of fuction may be made to satisfy any prescribed boundary conditions along the longitudinal edges. Hence, this will yield an exact solution to the governing differential equation.

General Equations

Coordinates and Displacements

Figure 1 shows the segment of a cylindrical shell with positive direction of coordinates x, y, and z. The displacements in the positive directions of x, y, and z are referred to as u, v, and w, respectively. The dimensions of the shell are given by length L, thickness t, radius to the middle surface R, half-width B, and half-subtended angle ψ_0.

General Equations

The Donnell's equations for a cylindrical shell subjected to an axial compression stress σ_x can be written as

$$\nabla^8 w + \frac{12z^2}{L^4}\frac{\partial^4 w}{\partial x^4} + \frac{\pi^2}{L^2}\nabla^4\left[K_x\frac{\partial^2 w}{\partial x^2}\right] = 0 \qquad (1)$$

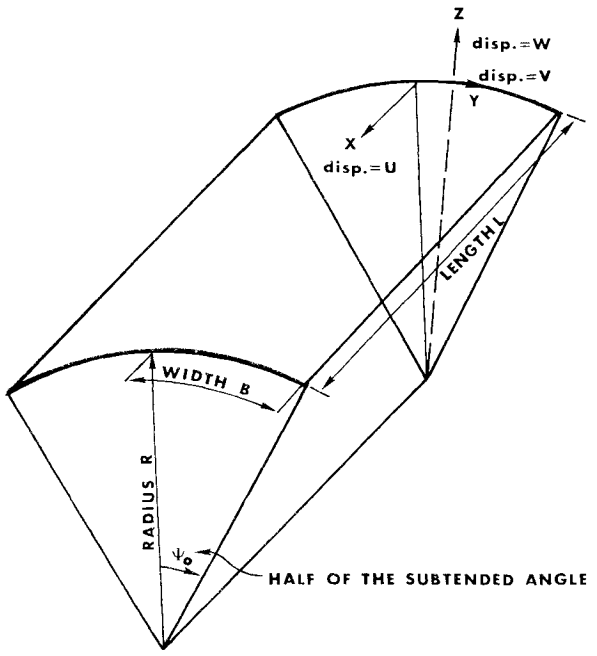

Fig. 1 Coordinates and displacements of a cylindrical shell.

where

$$K_x = \frac{\sigma_x t L^2}{D\pi^2}; \quad z = \frac{L^2}{Rt}(1-\mu^2)^{1/2}; \quad D = \frac{Et^3}{12(1-\mu^2)} \tag{2}$$

Solution for Shells Subjected to Uniform Compressive Stress

The shell is assumed to be simply supported at the ends $x = 0$ and $x = L$. Then along these ends

$$w = 0; \quad M_x = -D[\partial^2 w/\partial x^2 + \mu\,\partial^2 w/\partial y^2] = 0 \tag{3}$$

The following expression for w which satisfies the preceding two conditions is assumed in order to solve Eq. (1).

$$w = [a e^{\phi y}] \sin \alpha x \tag{4}$$

where

$$\alpha = m\pi/L, \qquad m = 1, 2, 3, \ldots \tag{5}$$

Substituting Eq. (4) into Eq. (1), the following indicial equation is obtained

$$\phi^8 - 4\alpha^2\phi^6 + \left(6 - \frac{K_x}{m^2}\right)\alpha^4\phi^4 + \left(-4 + \frac{2K_x}{m^2}\right)\alpha^6\phi^2 + \left[1 - \frac{K_x}{m^2} + \frac{12z^2}{m\pi^4}\right]\alpha^8 = 0 \tag{6}$$

Indicial Roots and Symmetrical and Antisymmetrical Deflection Patterns

The eight roots of Eq. (6) can be explicitly written as four sets of complex conjugates.

$$\phi = (\phi_1 \pm i\phi_2)\alpha, \quad (-\phi_1 \pm i\phi_2)\alpha, \quad (\phi_3 \pm i\phi_4)\alpha \quad \text{and} \quad (-\phi_3 \pm i\phi_4)\alpha \tag{7}$$

where

$$\left.\begin{matrix}\phi_1 \\ \phi_2\end{matrix}\right\} = \frac{1}{(2)^{1/2}}\left[\pm[1 + p(q+r)^{1/2}] + \{[1 + p(q+r)^{1/2}]^2 + [p(-q+r)^{1/2}]^2\}^{1/2}\right]^{1/2} \tag{8}$$

$$\left.\begin{matrix}\phi_3 \\ \phi_4\end{matrix}\right\} = \frac{1}{(2)^{1/2}}\left[\pm[1 - p(q+r)^{1/2}] + \{[1 - p(q+r)^{1/2}]^2 + [p(-q+r)^{1/2}]^2\}^{1/2}\right]^{1/2} \tag{9}$$

$$p = (3)^{1/2}\frac{L}{m\pi t}(1-\mu^2)^{1/2}; \quad q = \frac{\sigma_x}{E}; \quad r = \frac{t}{(3)^{1/2}R(1-\mu^2)^{1/2}} \tag{10}$$

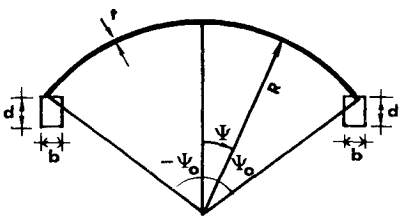

Fig. 2 Cylindrical shell with identical edge stiffeners.

If the value q is equal to r, it may be seen that ϕ_2 and ϕ_4 are equal to zero and therefore the differential equation will have repeated roots. In this paper, open shells having buckling stress less than or equal to classical value

$$\sigma_{cl} = \frac{1}{(3)^{1/2}(1-\mu^2)^{1/2}}\frac{Et}{R} \tag{11}$$

are examined. Hence, the form of roots given previously are valid for such cases.

$$w = [e^{\phi_1 \alpha y}(a_1 \sin \phi_2\alpha y + a_2 \cos \phi_2\alpha y) + e^{\phi_3 \alpha y}(a_3 \sin \phi_4\alpha y + a_4 \cos \phi_4\alpha y) + e^{-\phi_1 \alpha y}(a_5 \sin \phi_2\alpha y + a_6 \cos \phi_2\alpha y) + e^{-\phi_3 \alpha}y(a_7 \sin \phi_4\alpha y + a_8 \cos \phi_4 \alpha y)] \sin \alpha x \tag{12}$$

The expressions for u and v can be obtained from the uncoupled Donnell's equations.

For a shell with symmetrical boundary conditions and loadings, the shell may buckle either into a symmetrical or into an antisymmetrical deflection pattern. Hence it will be desirable to separate the symmetrical and antisymmetrical parts for u, v, w and the required stress resultants for numerical calculations. These are given in the Appendix.

Boundary Conditions

The two rectangular edge stiffeners located along the edges of the shell $y = \pm B$ (or $\psi = \psi_0$), are assumed to be of identical cross section $b \times d$ and oriented as shown in Fig. 2. The following boundary conditions are assumed for the stiffeners.

a) Twisting of the stiffeners is assumed to be negligible. This means that at $\psi = \pm\psi_0$, the rotation of the tangent to the arc of the shell will be equal to zero, or

$$\theta_B = \left[\frac{v}{R} - \frac{\partial w}{\partial y}\right]_{\psi = \pm\psi_0} = 0 \tag{13}$$

As the torsional rotation is assumed to be negligible, horizontal and vertical deflections at any point on the upper face of the edge beam, v_B and w_B, respectively, will be equal to horizontal and vertical deflections at the centroid of the beams $\bar{v}$ and $\bar{w}$, respectively, as shown in Fig. 3. Since energy due to torsional

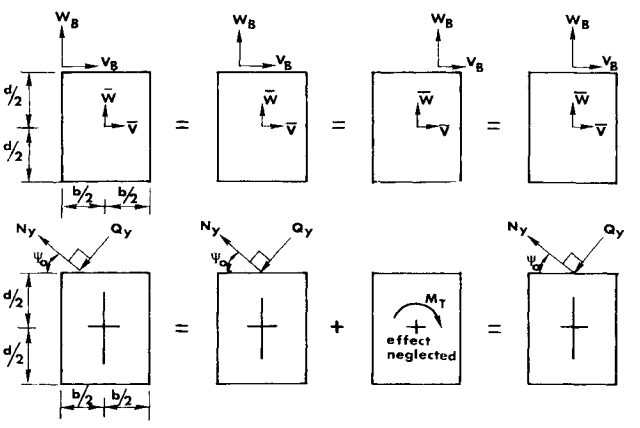

Fig. 3 Effect of neglecting the twisting of edge stiffeners.

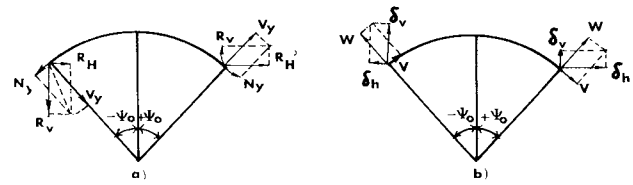

Fig. 4 Forces and displacement components at the longitudinal edges of a cylindrical shell with edge stiffeners.

moment is neglected, the solution for critical load will be valid, no matter whether the shell is connected at the midpoint or at any other point along the upper edge of the stiffener cross section. Therefore, in the following discussions, the shell will be assumed to be connected at the centerline of the upper face of the stiffener.

b) The edge stiffener is assumed to offer no lateral resistance, which implies that at $\psi = \pm\psi_0$ the horizontal reaction of the shell will be equal to zero. Then, from Fig. 4

$$[R_H]_{\psi=\pm\psi_0} = [N_y \cos\psi + V_y \sin\psi]_{\psi=\pm\psi_0} = 0 \qquad (14)$$

c) The longitudinal displacement u of the shell at $\psi = \pm\psi_0$ is equal to the longitudinal displacement at the upper face of the edge stiffener u_B, or

$$[u]_{\psi=\pm\psi_0} - [u_B]_{\psi=\pm\psi_0} = 0 \qquad (15)$$

d) The vertical displacement δ_v of the shell at $\psi = \pm\psi_0$ is equal to the vertical displacement of the edge stiffener $w_B = \bar{w}$ or, from Fig. 4

$$[\delta_v]_{\psi=\pm\psi_0} - [w_B]_{\psi=\pm\psi_0} = [w\cos\psi - v\sin\psi]_{\psi=\pm\psi_0} - [\bar{w}]_{\psi=\pm\psi_0} = 0 \qquad (16)$$

Other assumptions may be made with regard to the boundary conditions which will result in different expressions. However, the same procedure illustrated here can be followed for obtaining the critical buckling stress for other boundary conditions.

Coordinate Systems, Displacements, and Forces in the Edge Stiffeners

Referring to Fig. 5, the coordinate axis $\bar{x}$ coincides with the centroidal axis of the edge stiffener and is parallel to the x axis of the shell. The coordinate axis $\bar{y}$ passing through the centroid is horizontal and positive towards the right. The coordinate axis $\bar{z}$, passing through the centroid, is vertical and positive upward. The displacements along $\bar{x}$, $\bar{y}$, and $\bar{z}$ axis are $\bar{u}$, $\bar{v}$, and $\bar{w}$, respectively, and the corresponding displacements at the top of the stiffeners are u_B, v_B, and w_B, respectively. The resisting forces acting on the edge stiffeners are: axial force F_B (positive when it is in tension), shearing force V_B (positive when it is upward on the front face), and bending moment M_B (positive when it causes upward deflections). The loads acting on the stiffeners are forces opposite to the shell forces along the edges. Forces shown in Fig. 4 are for the right-side stiffener only. Loads on the left-side stiffener will be in the opposite directions.

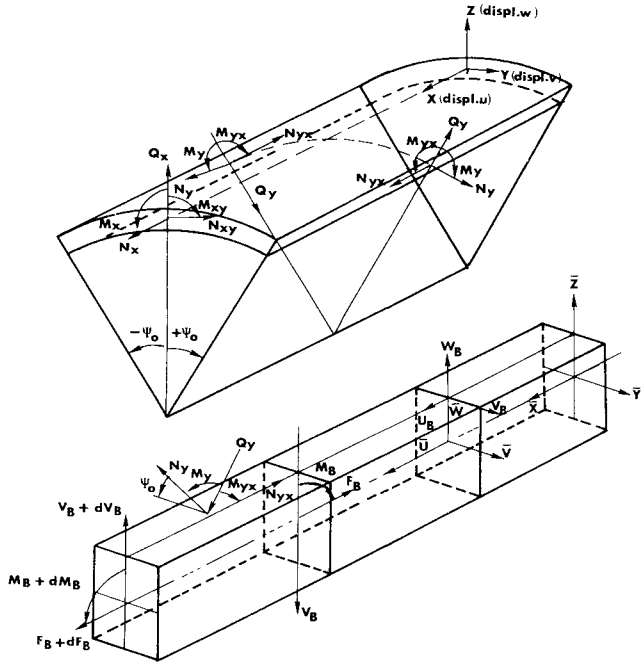

Fig. 5 Coordinate systems, displacement, and forces in shell and edge stiffeners.

Edge Stiffener Equations

Expressing

$$V_y = V_y' \sin\alpha x; \quad N_{yx} = N_{yx}' \cos\alpha x; \quad N_y = N_y' \sin\alpha x \qquad (17)$$

and using the equilibrium equations

$$\sum F_x = 0, \quad \sum F_{\bar{z}} = 0 \quad \text{and} \quad \sum M_{\bar{y}} = 0 \qquad (18)$$

the following edge equations for edge stiffeners can be derived:

$$[F_B]_{\psi=\pm\psi_0} = \mp[(1/\alpha)N_{yx}' \sin\alpha x]_{\psi=\pm\psi_0} \qquad (19)$$

$$[M_B]_{\psi=\pm\psi_0} = \pm\left[\left(\frac{1}{\alpha^2}V_y' \cos\psi - \frac{\alpha d}{2}N_{yx}' - N_y' \sin\psi\right)\sin\alpha x\right]_{\psi=\pm\psi_0} \qquad (20)$$

$$[\bar{w}]_{\psi=\pm\psi_0} = \pm\left[\frac{1}{\alpha^4 EI_B}\left(V_y' \cos\psi - \frac{\alpha d}{2}N_{yx}' - N_y' \sin\psi\right)\sin\alpha x\right]_{\psi=\pm\psi_0} \qquad (21)$$

$$[u_B]_{\psi=\pm\psi_0} = \mp\left[\left(\frac{4}{E\alpha^2 A_B}N_{yx}' - \frac{d}{2\alpha^3 EI_B}V_y' \cos\psi + \frac{d}{2\alpha^3 EI_B}N_y' \sin\psi\right)\sin\alpha x\right]_{\psi=\pm\psi_0} \qquad (22)$$

where

$$A_B = bd \quad \text{and} \quad I = bd^3/12 \qquad (23)$$

Final Boundary Equations

Substituting Eqs. (19–22) and equations for u, v, and w from the Appendix, using the symmetric and antisymmetric requirements on u, v, w, N_{xy}, and V_y two sets of four boundary equations are obtained. These are listed in the Appendix.

Calculation of Buckling Stress

The boundary equations (A10–A13) in the Appendix contain the 4 undetermined constants A_1 to A_4. These equations may be written in the following matrix form

$$\begin{bmatrix} C_{1,1} & C_{1,2} & C_{1,3} & C_{1,4} \\ C_{2,1} & C_{2,2} & C_{2,3} & C_{2,4} \\ C_{3,1} & C_{3,2} & C_{3,3} & C_{3,4} \\ C_{4,1} & C_{4,2} & C_{4,3} & C_{4,4} \end{bmatrix} \begin{bmatrix} A_1 \\ A_2 \\ A_3 \\ A_4 \end{bmatrix} = \begin{bmatrix} 0 \\ 0 \\ 0 \\ 0 \end{bmatrix} \qquad (24)$$

The critical values of compressive stress will be found by setting the determinant of matrix C of Eq. (24) to zero. In order to avoid large numbers, coefficients of A_1 and A_2 are multiplied by $e^{-\phi_1 \alpha B}$ and coefficients of A_3 and A_4 are multiplied by $e^{-\phi_3 \alpha B}$. This will not have any effect on the final results.

As the compressive stress is implicitly involved in all the determinant elements, any direct algebraic calculations for the critical stress is impossible. The critical stress is therefore obtained by numerical methods using an electronic computer.

For a given mode of buckling (symmetrical or antisymmetrical) and a given value of m, the sign of the value of the determinant may be obtained for any particular stress value. Starting from zero, the stress is progressively increased in small increments until the sign of the value of the determinant is changed. The change in sign indicates the presence of a buckling value between the previous value and the present value of stress. The interval of search is then narrowed until the desired degree of accuracy is

obtained. Buckling stresses for various values of m are determined for a given mode of buckling. The smallest buckling value for various values of m is the buckling stress for the given mode. The critical buckling stress is given by the smaller value of the buckling stress of the symmetrical mode and that for the antisymmetrical mode.

The validity of this approach is demonstrated by examining a shell with the following properties:

$$L/R = 10,\ t/R = 1/1000,\quad b/t = 0.2,\quad \psi_0 = 45^\circ$$

The buckling stress vs the t/d ratio is plotted in Fig. 5. In the case of antisymmetric buckling, $m = 1$ governs, whereas in the case of symmetric buckling, $m = 2$ governs. The critical buckling stress is given by the antisymmetric buckling case. The mode of buckling and the governing values of m for critical buckling stress agree with the values for a shell with free edges.[7]

Figure 6 shows that for a shell with deep edge stiffeners the buckling value can be as high as or higher than the cylinder value. Since the size of the edge stiffener required to give the cylinder buckling value is usually of primary interest, buckling values above the cylinder value are not investigated. However, it should be pointed out that there is no difficulty in determining the buckling values above the cylinder value, although their determination will involve changes of the characteristic roots given in Eq. ( ).

Figure 6 also shows that the critical buckling stress for a shell with very shallow edge stiffeners is well above the critical buckling stress of the shell with free edges. This may be because of the assumption that rotation is prevented along the longitudinal edges. The buckling stress for a shell with edge stiffeners of medium depth is only slightly above the buckling stress for the shell with free edges and is below the buckling stress for the shell with shallow edge stiffeners. It is surmised that a shell with edge stiffeners of moderate depth may behave like a shell with free longitudinal edges but with a larger central angle, the buckling stress of which may be equal to or slightly lower than the one with a smaller central angle.[7]

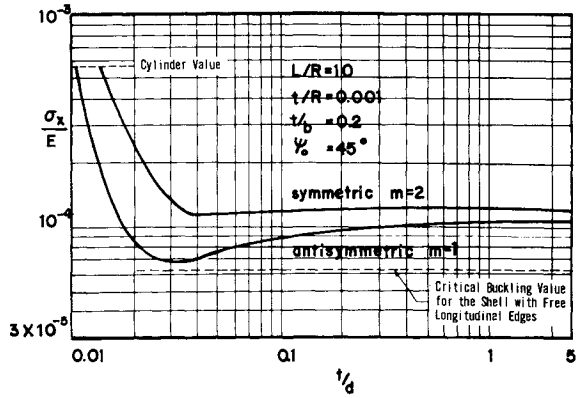

Fig. 6 Critical buckling load for a shell with edge stiffeners.

Appendix

Solutions for w, u, and v

With the subscript S referring to the symmetric part and the subscript A referring to the antisymmetric part, the final solutions for w, u, and v are given by the following equations:

$$\left.\begin{matrix} w_S \\ w_A \end{matrix}\right\} = [A_1(e^{\phi_1\alpha y} \pm e^{-\phi_1\alpha y})\sin\phi_2\alpha y + A_2(e^{\phi_1\alpha y} \pm e^{-\phi_1\alpha y})\cos\phi_2\alpha y + A_3(e^{\phi_3\alpha y} \mp e^{-\phi_3\alpha y})\sin\phi_4\alpha y + A_4(e^{\phi_3\alpha y} \pm e^{-\phi_3\alpha y})\cos\phi_4\alpha y]\sin\alpha x \tag{A1}$$

$$\left.\begin{matrix} u_S \\ u_A \end{matrix}\right\} = \{A_1[s_1(e^{\phi_1\alpha y} \mp e^{-\phi_1\alpha y})\sin\phi_2\alpha y + s_2(e^{\phi_1\alpha y} \pm e^{-\phi_1\alpha y})\cos\phi_2\alpha y] + A_2[s_1(e^{\phi_1\alpha y} \pm e^{-\phi_1\alpha y})\cos\phi_2\alpha y - s_2(e^{\phi_1\alpha y} \mp e^{-\phi_1\alpha y})\sin\phi_2\alpha y] + A_3[\bar{s}_1(e^{\phi_3\alpha y} \mp e^{-\phi_3\alpha y})\sin\phi_4\alpha y + \bar{s}_2(e^{\phi_3\alpha y} \pm e^{-\phi_3\alpha y})\cos\phi_4\alpha y] + A_4[\bar{s}_1(e^{\phi_3\alpha y} \pm e^{-\phi_3\alpha y})\cos\phi_4\alpha y - \bar{s}_2(e^{\phi_3\alpha y} \mp e^{-\phi_3\alpha y})\sin\phi_4\alpha y]\}\rho_1\cos\alpha x \tag{A2}$$

$$\left.\begin{matrix} v_S \\ v_A \end{matrix}\right\} = \{A_1[s_1'(e^{\phi_1\alpha y} \pm e^{-\phi_1\alpha y})\sin\phi_2\alpha y + s_2'(e^{\phi_1\alpha y} \mp e^{-\phi_1\alpha y})\cos\phi_2\alpha y] + A_2[s_1'(e^{\phi_1\alpha y} \mp e^{-\phi_1\alpha y})\cos\phi_2\alpha y - s_2'(e^{\phi_1\alpha y} \pm e^{-\phi_1\alpha y})\sin\phi_2\alpha y] + A_3[\bar{s}_1'(e^{\phi_3\alpha y} \pm e^{-\phi_3\alpha y})\sin\phi_4\alpha y + \bar{s}_2'(e^{\phi_3\alpha y} \mp e^{-\phi_3\alpha y})\cos\phi_4\alpha y] + A_4[\bar{s}_1'(e^{\phi_3\alpha y} \mp e^{-\phi_3\alpha y})\cos\phi_4\alpha y - \bar{s}_2'(e^{\phi_3\alpha y} \pm e^{-\phi_3\alpha y})\sin\phi_4\alpha y]\}\rho_1\sin\alpha x \tag{A3}$$

where

$$s_1 = p_1p_3 - p_2p_4 \qquad s_2 = p_1p_4 + p_2p_3$$
$$\bar{s}_1 = \bar{p}_1\bar{p}_3 - \bar{p}_2\bar{p}_4 \qquad \bar{s}_2 = \bar{p}_1\bar{p}_4 + \bar{p}_2\bar{p}_3$$
$$s_1' = p_1p_5 - p_2p_6 \qquad s_2' = p_1p_6 + p_2p_5$$
$$\bar{s}_1' = \bar{p}_1\bar{p}_5 - \bar{p}_2\bar{p}_6 \qquad \bar{s}_2' = \bar{p}_1\bar{p}_6 + \bar{p}_2\bar{p}_5$$
$$p_1 = 1 - 2(\phi_1^2 - \phi_2^2) + (\phi_1^4 - 6\phi_1^2\phi_2^2 + \phi_2^4) = 2p^2q$$
$$\bar{p}_1 = 1 - 2(\phi_3^2 - \phi_4^2) + (\phi_3^4 - 6\phi_3^2\phi_4^2 + \phi_4^4) = 2p^2q = p_1$$
$$p_2 = 4\phi_1\phi_2(1 - \phi_1^2 + \phi_2^2) = -2p^2(-q^2 + r^2)^{1/2}$$
$$\bar{p}_2 = 4\phi_3\phi_4(1 - \phi_3^2 + \phi_4^2) = 2p^2(-q^2 + r^2)^{1/2} = -p_2 \tag{A4}$$
$$p_3 = \mu + (\phi_1^2 - \phi_2^2) = (1 + \mu) + p(q + r)^{1/2}$$
$$\bar{p}_3 = \mu + (\phi_3^2 - \phi_4^2) = (1 + \mu) - p(q + r)^{1/2}$$
$$p_4 = 2\phi_1\phi_2 = p(-q + r)^{1/2}$$
$$\bar{p}_4 = 2\phi_3\phi_4 = p(-q + r)^{1/2} = p_4$$
$$p_5 = \phi_1[(2 + \mu) - (\phi_1^2 - 3\phi_2^2)]$$
$$\bar{p}_5 = \phi_3[(2 + \mu) - (\phi_3^2 - 3\phi_4^2)]$$
$$p_6 = \phi_2[(2 + \mu) - (3\phi_1^2 - \phi_2^2)]$$
$$\bar{p}_6 = \phi_4[(2 + \mu) - (3\phi_3^2 - \phi_4^2)]$$
$$\rho_1 = \frac{1}{\alpha R}\frac{1}{4p^4r^2}$$

$$4p^4r^2 = p_1^2 + p_2^2 = \bar{p}_1^2 + \bar{p}_2^2 = \frac{12(1-\mu^2)}{m\pi^4}\left(\frac{L}{t}\right)^2\left(\frac{L}{R}\right)^2$$

Solution of M_y, N_{xy}, N_y, and V_y

Using the equations for u, v, and w, the solution of M_y, N_{xy}, N_y, and V_y can be written as follows:

$$\left.\begin{matrix} (M_y)_S \\ (M_y)_A \end{matrix}\right\} = \{A_1[p_7(e^{\phi_1\alpha y} \mp e^{-\phi_1\alpha y})\sin\phi_2\alpha y + p_4(e^{\phi_1\alpha y} \pm e^{\phi_1\alpha y})\cos\phi_2\alpha y] + A_2[p_7(e^{\phi_1\alpha y} \pm e^{-\phi_1\alpha y})\cos\phi_2\alpha y - p_4(e^{\phi_1\alpha y} \mp e^{-\phi_1\alpha y})\sin\phi_2\alpha y] + A_3[\bar{p}_7(e^{\phi_3\alpha y} \mp e^{-\phi_3\alpha y})\sin\phi_4\alpha y + \bar{p}_4(e^{\phi_3\alpha y} \pm e^{-\phi_3\alpha y})\cos\phi_4\alpha y] + A_4[\bar{p}_7(e^{\phi_3\alpha y} \pm e^{-\phi_3\alpha y})\cos\phi_4\alpha y - \bar{p}_4(e^{\phi_3\alpha y} \mp e^{-\phi_3\alpha y})\sin\phi_4\alpha y]\}\rho_2\sin\alpha x \tag{A5}$$

$$\left.\begin{matrix} (N_{xy})_S \\ (N_{xy})_A \end{matrix}\right\} = \{A_1[q_1(e^{\phi_1\alpha y} \pm e^{-\phi_1\alpha y})\sin\phi_2\alpha y + q_2(e^{\phi_1\alpha y} \mp e^{-\phi_1\alpha y})\cos\phi_2\alpha y] + A_2[q_1(e^{\phi_1\alpha y} \mp e^{-\phi_1\alpha y})\cos\phi_2\alpha y - q_2(e^{\phi_1\alpha y} \pm e^{-\phi_1\alpha y})\sin\phi_2\alpha y] + A_3[\bar{q}_1(e^{\phi_3\alpha y} \pm e^{-\phi_3\alpha y})\sin\phi_4\alpha y + \bar{q}_2(e^{\phi_3\alpha y} \mp e^{-\phi_3\alpha y})\cos\phi_4\alpha y] + A_4[\bar{q}_1(e^{\phi_3\alpha y} \mp e^{-\phi_3\alpha y})\cos\phi_4\alpha y - \bar{q}_2(e^{\phi_3\alpha y} \pm e^{-\phi_3\alpha y})\sin\phi_4\alpha y]\}\rho_3\cos\alpha x \tag{A6}$$

$$\left.\begin{matrix}(N_y)_S\\(N_y)_A\end{matrix}\right\} = \{A_1[p_1(e^{\phi_1\alpha y}\mp e^{-\phi_1\alpha y})\sin\phi_2\alpha y+ p_2(e^{\phi_1\alpha y}\pm e^{\phi_1\alpha y})\cos\phi_2\alpha y]+ A_2[p_1(e^{\phi_1\alpha y}\pm e^{-\phi_1\alpha y})\cos\phi_2\alpha y- p_2(e^{\phi_1\alpha y}\mp e^{-\phi_1\alpha y})\sin\phi_2\alpha y]+ A_3[\bar{p}_1(e^{\phi_3\alpha y}\mp e^{-\phi_3\alpha y})\sin\phi_4\alpha y+ \bar{p}_2(e^{\phi_3\alpha y}\pm e^{-\phi_3\alpha y})\cos\phi_4\alpha y]+ A_4[\bar{p}_1(e^{\phi_3\alpha y}\pm e^{-\phi_3\alpha y})\cos\phi_4\alpha y- \bar{p}_2(e^{\phi_3\alpha y}\mp e^{-\phi_3\alpha y})\sin\phi_4\alpha y]\}\rho_3\sin\alpha x \tag{A7}$$

$$\left.\begin{matrix}(V_y)_S\\(V_y)_A\end{matrix}\right\} = \{A_1[p_8(e^{\phi_1\alpha y}\pm e^{-\phi_1\alpha y})\sin\phi_2\alpha y+ p_9(e^{\phi_1\alpha y}\mp e^{-\phi_1\alpha y})\cos\phi_2\alpha y]+ A_2[p_8(e^{\phi_1\alpha y}\mp e^{-\phi_1\alpha y})\cos\phi_2\alpha y- p_9(e^{\phi_1\alpha y}\pm e^{-\phi_1\alpha y})\sin\phi_2\alpha y]+ A_3[\bar{p}_8(e^{\phi_3\alpha y}\pm e^{-\phi_3\alpha y})\sin\phi_4\alpha y+ \bar{p}_9(e^{\phi_3\alpha y}\mp e^{-\phi_3\alpha y})\cos\phi_4\alpha y]+ A_4[\bar{p}_8(e^{\phi_3\alpha y}\mp e^{-\phi_3\alpha y})\cos\phi_4\alpha y- \bar{p}_9(e^{\phi_3\alpha y}\pm e^{-\phi_3\alpha y})\sin\phi_4\alpha y]\}\alpha\rho_2\sin\alpha x \tag{A8}$$

where

$$\left.\begin{aligned} p_7 &= \phi_1{}^2-\phi_2{}^2-\mu \\ \bar{p}_7 &= \phi_3{}^2-\phi_4{}^2-\mu \\ p_8 &= \phi_1(\phi_1{}^2-3\phi_2{}^2-2+\mu) \\ \bar{p}_8 &= \phi_3(\phi_3{}^2-3\phi_4{}^2-2+\mu) \\ p_9 &= \phi_2(3\phi_1{}^2-\phi_2{}^2-2+\mu) \\ \bar{p}_9 &= \phi_4(3\phi_3{}^2-\phi_4{}^2-2+\mu) \\ \rho_2 &= -\frac{\alpha^2Et^3}{12(1-\mu^2)} \qquad \rho_3 = \frac{Et}{R}\frac{1}{4p^4r^2} \\ q_1 &= p_1\phi_1-p_2\phi_2 \qquad \bar{q}_1 = \bar{p}_1\phi_3-\bar{p}_2\phi_4 \\ q_2 &= p_1\phi_2+p_2\phi_1 \qquad \bar{q}_2 = \bar{p}_1\phi_4+\bar{p}_2\phi_3 \end{aligned}\right\} \tag{A9}$$

$$\begin{bmatrix}(\theta_B)_S\\(\theta_B)_A\end{bmatrix}_{\psi=\pm\psi_0} = \Big\{(e^{\phi_1\alpha B}\pm e^{-\phi_1\alpha B})[\rho s_1{}'-\phi_1]\sin\phi_2\alpha y+ (e^{\phi_1\alpha B}\mp e^{-\phi_1\alpha B})[\rho s_2{}'-\phi_2]\cos\phi_2\alpha y\Big\}\begin{matrix}A_{1_S}\\A_{1_A}\end{matrix}+ \Big\{(e^{\phi_1\alpha B}\mp e^{-\phi_1\alpha B})[\rho s_1{}'-\phi_1]\cos\phi_2\alpha y- (e^{\phi_1\alpha B}\pm e^{-\phi_1\alpha B})[\rho s_2{}'-\phi_2]\sin\phi_2\alpha y\Big\}\begin{matrix}A_{1_S}\\A_{2_S}\end{matrix}+ \Big\{(e^{\phi_3\alpha B}\pm e^{-\phi_3\alpha B})[\rho\bar{s}_1{}'-\phi_3]\sin\phi_4\alpha y+ (e^{\phi_3\alpha B}\mp e^{-\phi_3\alpha B})[\rho\bar{s}_2{}'-\phi_4]\cos\phi_4\alpha y\Big\}\begin{matrix}A_{3_S}\\A_{3_A}\end{matrix}+ \Big\{(e^{\phi_3\alpha B}\mp e^{-\phi_3\alpha B})[\rho\bar{s}_1{}'-\phi_3]\cos\phi_4\alpha y- (e^{\phi_3\alpha B}\pm e^{-\phi_3\alpha B})[\rho\bar{s}_2{}'-\phi_4]\sin\phi_4\alpha y\Big\}\begin{matrix}A_{4_S}=0\\A_{4_A}\end{matrix} \tag{A10}$$

$$\begin{bmatrix}(R_H)_S\\(R_H)_A\end{bmatrix}_{\psi=\pm\psi_0} = \Big[(e^{\phi_1\alpha B}\mp e^{-\phi_1\alpha B})(\alpha R\rho_1\cos\psi_0\sin\phi_2\alpha B- p_9\sin\psi_0\cos\phi_2\alpha B)+(e^{\phi_1\alpha B}\pm e^{-\phi_1\alpha B})\times (\alpha R\rho_2\cos\psi_0\cos\phi_2\alpha B-p_8\sin\psi_0\sin\phi_2\alpha B)\Big]\begin{matrix}A_{1_S}\\A_{1_A}\end{matrix}+ \Big[(e^{\phi_1\alpha B}\pm e^{-\phi_1\alpha B})(\alpha R\rho_1\cos\psi_0\cos\phi_2\alpha B+ p_8\sin\psi_0\sin\phi_2\alpha B)-(e^{\phi_1\alpha B}\mp e^{-\phi_1\alpha B})\times (\alpha R\rho_2\cos\psi_0\sin\phi_2\alpha B+p_9\sin\psi_0\cos\phi_2\alpha B)\Big]\begin{matrix}A_{2_S}\\A_{2_A}\end{matrix}+$$

$$\Big[(e^{\phi_3\alpha B}\mp e^{-\phi_3\alpha B})(\alpha R\bar{\rho}_1\cos\psi_0\sin\phi_4\alpha B- \bar{p}_9\sin\psi_0\cos\phi_4\alpha B)+(e^{\phi_3\alpha B}\pm e^{-\phi_3\alpha B})\times (\alpha R\bar{\rho}_2\cos\psi_0\cos\phi_4\alpha B-\bar{p}_8\sin\psi_0\sin\phi_4\alpha B)\Big]\begin{matrix}A_{3_S}\\A_{3_A}\end{matrix}+ \Big[(e^{\phi_3\alpha B}\pm e^{-\phi_3\alpha B})(\alpha R\bar{\rho}_1\cos\psi_0\cos\phi_4\alpha B+ \bar{p}_8\sin\psi_0\sin\phi_4\alpha B)-(e^{\phi_3\alpha B}\mp e^{-\phi_3\alpha B})\times (\alpha R\bar{\rho}_2\cos\psi_0\sin\phi_4\alpha B+\bar{p}_9\sin\psi_0\cos\phi_4\alpha B)\Big]\begin{matrix}A_{4_S}=0\\A_{4_A}\end{matrix} \tag{A11}$$

$$\begin{bmatrix}u_S-(u_B)_S\\u_A-(u_B)_A\end{bmatrix}_{\psi=\pm\psi_0} = \Big\{\big[e^{\phi_1\alpha B}\mp e^{-\phi_1\alpha B}\big]\times [(K_1s_1+K_4p_1)\sin\phi_2\alpha B+(K_2q_2+K_3p_9)\cos\phi_2\alpha B]+ [e^{\phi_1\alpha B}\pm e^{-\phi_1\alpha B}][(K_2q_1+K_3p_8)\sin\phi_2\alpha B+ (K_1s_2+K_4p_2)\cos\phi_2\alpha B]\Big\}\begin{matrix}A_{1_S}\\A_{1_A}\end{matrix}+ \Big\{[e^{\phi_1\alpha B}\pm e^{-\phi_1\alpha B}][(K_1s_1+K_4p_1)\cos\phi_2\alpha B- (K_2q_2+K_3p_9)\sin\phi_2\alpha B]+[e^{\phi_1\alpha B}\mp e^{-\phi_1\alpha B}]\times [(K_2q_1+K_3p_8)\cos\phi_2\alpha B-(K_1s_2+K_4p_2)\sin\phi_2\alpha B]\Big\}\begin{matrix}A_{2_S}\\A_{2_A}\end{matrix}+ \Big\{[e^{\phi_3\alpha B}\mp e^{-\phi_3\alpha B}][(K_1\bar{s}_1+K_4\bar{p}_1)\sin\phi_4\alpha B+ (K_2\bar{q}_2+K_3\bar{p}_9)\cos\phi_4\alpha B]+[e^{\phi_3\alpha B}\pm e^{-\phi_3\alpha B}]\times [(K_2\bar{q}_1+K_3\bar{p}_8)\sin\phi_4\alpha B+(K_1\bar{s}_2+K_4\bar{p}_2)\cos\phi_4\alpha B]\Big\}\begin{matrix}A_{3S}\\A_{3A}\end{matrix}+ \Big\{[e^{\phi_3\alpha B}\pm e^{-\phi_3\alpha B}][(K_1\bar{s}_1+K_4\bar{p}_1)\cos\phi_4\alpha B- (K_2\bar{q}_2+K_3\bar{p}_9)\sin\phi_4\alpha B]+[e^{\phi_3\alpha B}\mp e^{-\phi_3\alpha B}]\times [(K_2\bar{q}_1+K_3\bar{p}_8)\cos\phi_4\alpha B-(K_1\bar{s}_2+K_4\bar{p}_2)\sin\phi_4\alpha B]\Big\}\begin{matrix}A_{4_S}=0\\A_{4_A}\end{matrix} \tag{A12}$$

$$\begin{bmatrix}(\delta_v)_S-\bar{w}_S\\(\delta_v)_A-\bar{w}_A\end{bmatrix}_{\psi=\pm\psi_0} = \Big\{\big[e^{\phi_1\alpha B}\mp e^{-\phi_1\alpha B}\big]\times [(K_5+K_9p_1)\sin\phi_2\alpha B+(K_6s_2{}'+K_7q_2+K_8p_9)\cos\phi_2\alpha B]+ [e^{\phi_1\alpha B}\pm e^{-\phi_1\alpha B}][(K_6s_1{}'+K_7q_1+K_8p_8)\sin\phi_2\alpha B+ K_9p_2\cos\phi_2\alpha B]\Big\}\begin{matrix}A_{1_S}\\A_{1_A}\end{matrix}+ \Big\{[e^{\phi_1\alpha B}\pm e^{-\phi_1\alpha B}][(K_5+K_9p_1)\cos\phi_2\alpha B- (K_6s_2{}'+K_7q_2+K_8p_9)\sin\phi_2\alpha B]+[e^{\phi_1\alpha B}\mp e^{-\phi_1\alpha B}]\times [(K_6s_1{}'+K_7q_1+K_8p_8)\cos\phi_2\alpha B-K_9p_2\sin\phi_2\alpha B]\Big\}\begin{matrix}A_{2_S}\\A_{2_A}\end{matrix}+ \Big\{[e^{\phi_3\alpha B}\mp e^{-\phi_3\alpha B}][(K_5+K_9p_1)\sin\phi_4\alpha B+ (K_6\bar{s}_2{}'+K_7\bar{q}_2+K_8\bar{p}_9)\cos\phi_4\alpha B]+[e^{\phi_3\alpha B}\pm e^{-\phi_3\alpha B}]\times [(K_6\bar{s}_1{}'+K_7\bar{q}_1+K_8\bar{p}_8)\sin\phi_4\alpha B+K_9\bar{p}_2\cos\phi_4\alpha B]\Big\}\begin{matrix}A_{3_S}\\A_{3_A}\end{matrix}+ \Big\{[e^{\phi_3\alpha B}\pm e^{-\phi_3\alpha B}][(K_5+K_9\bar{p}_1)\cos\phi_4\alpha B- (K_6\bar{s}_2{}'+K_7\bar{q}_2+K_8\bar{p}_9)\sin\phi_4\alpha B]+[e^{\phi_3\alpha B}\mp e^{-\phi_3\alpha B}]\times [(K_6\bar{s}_1{}'+K_7\bar{q}_1+K_8\bar{p}_8)\cos\phi_4\alpha B-K_9\bar{p}_2\sin\phi_4\alpha B]\Big\}\begin{matrix}A_{3_S}=0\\A_{3_A}\end{matrix} \tag{A13}$$

where

$$\left.\begin{aligned}
K_1 &= \frac{(m\pi)^3}{12(1-\mu^2)}\left(\frac{t}{L}\right)^2\left(\frac{R}{L}\right) \qquad p = \frac{(m\pi)^2}{12(1-\mu^2)}\left(\frac{t}{L}\right)^2 \\
K_2 &= \frac{(m\pi)^2}{3(1-\mu^2)}\left(\frac{t}{L}\right)\left(\frac{t}{b}\right)\left(\frac{t}{d}\right)\left(\frac{R}{L}\right) \\
K_3 &= \frac{1}{2(1-\mu^2)}\left(\frac{t}{d}\right)^2\left(\frac{t}{b}\right)\cos\psi_0 \\
K_4 &= \frac{(m\pi)^2}{2(1-\mu^2)}\left(\frac{t}{d}\right)^2\left(\frac{t}{b}\right)\left(\frac{R}{L}\right)\sin\psi_0 \qquad K_5 = \cos\psi_0 \\
K_6 &= -\frac{(m\pi)^3}{12(1-\mu^2)}\left(\frac{t}{L}\right)^2\left(\frac{R}{L}\right)\sin\psi_0 \\
K_7 &= \frac{m\pi}{2(1-\mu^2)}\left(\frac{t}{d}\right)^2\left(\frac{t}{b}\right)\left(\frac{R}{L}\right) \\
K_8 &= \frac{1}{(m\pi)(1-\mu^2)}\left(\frac{L}{t}\right)\left(\frac{t}{b}\right)\left(\frac{t}{d}\right)^3\cos\psi_0 \\
K_9 &= \frac{1}{(1-\mu^2)}\left(\frac{t}{d}\right)^3\left(\frac{t}{b}\right)\left(\frac{R}{t}\right)\sin\psi_0
\end{aligned}\right\} \quad \text{(A14)}$$

References

[1] Fung, Y. C. and Sechler, E. E., "Instability of Thin Elastic Shells," *Structural Mechanics, Proceedings of the First Symposium on Naval Structural Mechanics*, Pergamon Press, New York, 1960.

[2] Flügge, W., *Handbook of Engineering Mechanics*, McGraw-Hill, New York, 1962.

[3] Gerard, G. and Becker, H., *Handbook of Structural Stability*, Party III: "Buckling of Curved Plates and Shells," TN 3783, 1957, NACA.

[4] Gerard, G., *Handbook of Structral Stability*, Supplement to Part III, "Buckling of Curved Plates and Shells," TN D-163, 1959, NACA.

[5] Batdorf, S. B., "A Simplified Method of Elastic Stability Analysis for Thin Cylindrical Shells," Rept. 874, 1947, NACA.

[6] Leggett, D. M. A., "The Elastic Stability of a Long and Slightly Bent Rectangular Plate under Uniform Shear," *Proceedings of the Royal Society of London*, Ser. A, Vol. 162, 1937, p. 62.

[7] Chu, K. H. and Krishnamoorthy, G., "Buckling of Open Cylindrical Shells," *Proceedings of ASCE, Journal of the Engineering Mechanics Division*, Vol. 93, No. EM 2, April 1967.

[8] Donnell, L. H., "Stability of Thin Walled Tubes under Torsion," Rept. 479, 1933, NACA.

OCTOBER 1974 AIAA JOURNAL VOL. 12, NO. 10

Flowfield Measurements in an Asymmetric Axial Corner at $M = 12.5$

JAMES R. COOPER* AND WILBUR L. HANKEY JR.†
Aerospace Research Laboratories, Wright-Patterson Air Force Base, Ohio

A detailed study of shock-wave boundary-layer interaction and interference heating of an axial corner typical of vehicle junctions has been made. Extensive impact pressure profiles were obtained in addition to static pressure information and oil flow studies. Measurements revealed two large vortices within the boundary layer responsible for high local heating. A complex inviscid shock pattern dominated by a triple point structure was also determined.

Nomenclature

h = heat-transfer coefficient (Btu/ft^2-sec-°F)
M = Mach number
p = static pressure
p_I = impact pressure
R = flow reattachment location
S = flow separation location
Y = conical y value normalized with respect to x
Z = conical z value normalized with respect to x
ξ = static pressure ratio

Subscripts

c = cross flow component
T = values related to triple point

Presented as Paper 73-676 at the AIAA 6th Fluid and Plasma Dynamics Conference, Palm Springs, Calif., July 16–18, 1973; submitted July 26, 1973; revision received May 16, 1974.

Index categories: Boundary Layers and Convective Heat Transfer—Laminar; Jets, Wakes, and Viscid-Inviscid Flow Interactions; Supersonic and Hypersonic Flow.

* Captain, U.S. Air Force, Hypersonic Research Laboratory.

† Senior Scientist, Hypersonic Research Laboratory. Member AIAA.

Introduction

IN the design of an aerodynamic body subject to hypersonic flow it is important to understand the nature of the flowfield that will develop around the body. One of the most important reasons for understanding the flow is due to its high heating potential, not only in stagnation regions, but near flow interference regions as well. Often in hypersonic flow bow shocks generated by various portions of a configuration will trigger boundary-layer flow separation. The separated flow, after negotiating the adverse pressure gradient presented by the shock, will attach itself to the surface and cause heating rates at reattachment which can sometimes exceed those at the leading edge stagnation regions. Without adequate knowledge of this three-dimensional separation and reattachment phenomena and its associated heating capability, a design may not properly account for the higher heating rates and subsequent structural failure could occur.

One of the more common configurations that cause shock-induced boundary-layer separation is the axial corner, typically occurring on a vehicle at such locations as the wing body, body tail, or inlet junctions. Strong bow shocks are generated by the surfaces of an axial corner. The bow shock generated by one surface impinges on the boundary layer of the second surface